

1 **Genetic diversity decreases toward species range edges**

2 Chloé Schmidt<sup>1,2,\*</sup>, Jussi Mäkinen<sup>3</sup>, Jean-Philippe Lessard<sup>4</sup>, Colin J Garroway<sup>5</sup>

3 <sup>1</sup> Department of Biology, Dalhousie University; Halifax, B3H 4R2, Canada

4 <sup>2</sup> German Centre for Integrative Biodiversity Research (iDiv) Halle-Jena-Leipzig; Leipzig,  
5 04103, Germany

6 <sup>3</sup> Research Center for Ecological Change, Faculty of Biological and Environmental Sciences,  
7 University of Helsinki; Helsinki, Finland

8 <sup>4</sup> Department of Biology, Concordia University; Montréal, H4B 1R6, Canada

9 <sup>5</sup> Department of Biological Sciences, University of Manitoba; Winnipeg, R2T 2N2, Canada

10 \*Correspondence: [chloe.schmidt@dal.ca](mailto:chloe.schmidt@dal.ca)

11

12

13 **Abstract**

14 Changing species distributions amidst global change underscores a pressing need to better  
15 understand the processes that cause range limits. However, despite over a century of work, there  
16 is no consensus regarding whether there are generalizable contributors to the emergence of  
17 species range limits. Species' geographic distributions frequently taper without obvious physical  
18 or environmental barriers, raising a fundamental question about whether evolutionary processes  
19 contribute to the emergence of species range limits species. Theoretical models suggest that  
20 spatial variation in the strength of genetic drift can reduce the efficiency of natural selection to  
21 the point where range limits form. The extent to which this theory holds in real-world  
22 populations is uncertain. With data comprising 37,397 genotypes sampled across 59 mammal  
23 species' ranges from 1,271 sample sites, we show that effective population size and genetic  
24 diversity decline toward range edges, while genetic differentiation increases, indicating stronger  
25 drift and reduced gene flow in peripheral populations. These results demonstrate that limits to  
26 range expansion arise predictably as populations become small and isolated, which reduces the  
27 efficiency of natural selection. Our findings point to genetic drift as a general mechanism  
28 constraining range expansion, helping to explain the widespread structure of species'  
29 distributions and help explain commonly observed idiosyncratic patterns of range configuration  
30 and the organization of biodiversity.

31

## 32 **Introduction**

33 No species occurs everywhere. While species' range limits sometimes align with physical  
34 barriers or abrupt changes in environmental conditions, they also commonly taper off gradually.  
35 The emergence of tapering range edges is puzzling from an evolutionary perspective. Given  
36 sufficient time and genetic variation, theory predicts that populations should be capable of  
37 adapting in response to changing environments, including adaptive expansions into neighboring  
38 habitats<sup>1-5</sup>. Indeed, most populations experience strong selection throughout their ranges where  
39 they persist and often become locally adapted<sup>6</sup>. Populations can typically withstand or respond to  
40 selection pressures within their ranges. However, the ubiquity of range edges without clear  
41 physical barriers suggests that general evolutionary mechanisms limit adaptation at these  
42 margins.

43  
44 Theoretical models of range edge evolution are well-developed and point to the potential  
45 importance of genetic drift as an evolutionary contributor to range edge formation<sup>5,7-9</sup>. This  
46 theoretical work is compelling because of its simplicity and potential generality. All populations  
47 experience genetic drift—the collective contribution of random influences on allele frequency  
48 changes from one generation to the next—which erodes genetic diversity over time in proportion  
49 to their effective population size<sup>10</sup>. The effective population size of a population decreases as  
50 abundance and gene flow between populations decrease, thereby increasing the strength of  
51 genetic drift. Foundational population genetic theory demonstrates that as allele frequency  
52 change becomes increasingly stochastic, the efficiency of the deterministic process of natural  
53 selection declines<sup>11,12</sup>. The inverse relationship between drift and the efficiency of selection is  
54 also well supported empirically in vertebrates, where, for example, signatures of selection at

55 protein coding genes across the genome become increasingly apparent as effective population  
56 sizes become larger<sup>13</sup>.

57

58 In theory, all that is required for range edge formation is that effective population sizes decline  
59 toward range edges to the point where genetic drift overwhelms the efficiency of natural

60 selection and populations become less likely to persist, adapt, and expand (Fig. 1). Genetic drift  
61 can be a general process influencing range limits because drift-mediated limits to the efficiency  
62 of natural selection are independent of the strength of selection acting on particular phenotypes.

63 The fact that genetic drift reduces the efficiency of natural selection acting across all traits

64 simultaneously means that drift-mediated reductions in the efficiency of selection can contribute

65 to the formation of range edges regardless of specific traits or environmental contexts, which will

66 vary in detail across species, populations, and through time<sup>5,11</sup>. It also means that we can test the

67 contribution of drift-mediated limits to natural selection to range edge formation using simple

68 measures of genetic drift (i.e., effective population size) estimated at multiple points across a

69 species range<sup>14</sup>. Empirically, even if genetic drift is a general contributor to range edge

70 formation, we can be certain that genetic drift will be one among many other, likely more

71 idiosyncratic and context-specific, contributors to the emergence of range edges.

72

73 Although theoretical models strongly suggest that genetic drift is likely important for the

74 emergence and maintenance of range edges across species, empirical evidence supporting the

75 prevalence of this pattern in nature is limited (see <sup>15</sup>). We tested whether edge populations

76 experience stronger genetic drift than populations near the range interior by quantifying effective

77 population size, genetic diversity, and genetic differentiation at multiple locations across the

78 ranges of multiple species. Effective population size estimates the strength of genetic drift, which

79 should be reflected in reduced genetic diversity. Due to increasing geographic isolation, small  
80 edge populations receiving lower gene flow should also become increasingly genetically  
81 differentiated and experience stronger drift (Fig. 1). Leveraging open-source genetic data for  
82 terrestrial mammals worldwide, we quantified these genetic metrics for 1,271 local populations  
83 comprising 37,397 individuals sampled across 59 species of mammals scattered across regions of  
84 the world (Fig. 2, S1-2, Table S1).

85

## 86 **Results**

87 Consistent with predictions for drift-mediated limits to selection, spatially and phylogenetically  
88 explicit Bayesian generalized linear mixed models indicated that effective population sizes  
89 declined nearer to range edges for most species, pointing to a general pattern of stronger drift at  
90 range margins (Table 1, Table S2, Fig. 3, Figs. S2-5). We also found lower genetic diversity  
91 closer to the range edge, in terms of both the abundance and evenness of alleles (allelic richness  
92 and gene diversity, respectively) in local populations (Table 1, Table S2, Fig. 3, Figs. S2-5). This  
93 is the predicted consequence of increased genetic drift. Finally, populations near edges also  
94 tended to be more genetically distinct compared to populations further from edges, suggesting  
95 that reduced effective population size at the edge is also in part due to reduced gene flow (Table  
96 1, Table S2, Fig. 3, Figs. S2-5). Our findings of repeated, consistent patterns of spatial variation  
97 in the strength of genetic drift<sup>5,9,16</sup> and their consequences for the efficiency of natural selection  
98 emphasizes the potential importance of limits on the process of adaptation itself relative to the  
99 outcome of specific selection pressures<sup>11,12,17</sup>. That effective population sizes, genetic diversity,  
100 and gene flow declined toward range edges across a globally distributed sample of species  
101 provides compelling support for an important and generalizable role for genetic drift-mediated  
102 limits on genetic adaptation shaping range edges across species and localities.

### 103 **Reconciling ecological and evolutionary perspectives on range edge formation**

104 One of the best developed explanations for the emergence of range edges, the abundant center or  
105 central-marginal hypothesis, is agnostic about the reasons why species do not expand their  
106 geographical distribution through adaptive evolution at range margins. The abundant center  
107 hypothesis focuses on species ecology and posits that population sizes should peak in the center  
108 of the range where environmental conditions (including biotic and abiotic factors) best match  
109 species' needs, and decline toward edges as environments become less well suited to species'  
110 ecological needs<sup>18</sup>. However, it has become increasingly clear that the dynamics of populations  
111 in range interiors are complex and difficult to generalize<sup>15,19–29</sup>. Regions of high abundance  
112 within ranges often seem to be poorly aligned with geographic range centers, and species can  
113 have multiple abundance peaks across their range<sup>19,20,25</sup>. However, abundant center demographic  
114 patterns predict parallel variation in the intensity of drift, and thus decreased genetic diversity  
115 and increased population differentiation nearer range edges<sup>5,9</sup>. We explored support for the  
116 abundant center assumption with our data by fitting similar models using a local population's  
117 distance from the geographic range center rather than distance from a range edge. We found  
118 similar, but less clear results (Fig. S6), suggesting that distance from the geographic range center  
119 can act as a proxy for the range edge-based processes tested here.

120 We further explored the abundant center assumption by visualizing the positions of genetically  
121 diverse, well-connected core populations. From a population genetics perspective, population  
122 cores—wherever they occur in a range—should be characterized by high levels of gene flow and  
123 genetic diversity (Fig. 1). To do this, we mapped spatial genetic structure using pairwise  $F_{ST}$ <sup>30</sup>  
124 and population-specific  $F_{ST}$ <sup>31,32</sup> for the subset of species with the best geographic sampling  
125 across ranges (Fig. 4, S7, See SI Methods). Our maps of spatial genetic structure suggest that  
126 genetic core populations often encompass a large proportion of a species range, suggesting that

127 range interior dynamics tend not to be well-characterized by a single, abundant, centrally located  
128 core population.

129 The abundant center concept also contributes to an alternative evolutionary explanation for range  
130 edge emergence known as genetic swamping. Due to their higher abundance, central populations  
131 could be net producers of immigrants, and edge populations net recipients, generating density-  
132 dependent dispersal toward range edges<sup>33</sup>. Genetic swamping refers to the idea that migrants to  
133 edge populations that are locally adapted to central environmental conditions would reduce the  
134 mean fitness in edge populations and limit adaptive expansion into neighboring environments. A  
135 growing consensus supported by theory, experimentation, and observational data suggests that  
136 central-marginal patterns of gene flow tend to have neutral<sup>22</sup> or net positive effects on the mean  
137 fitness of edge populations due to added genetic diversity<sup>22,34</sup>. This suggests that rather than  
138 contributing to the emergence of range edges, gene flow to range margins typically facilitates  
139 adaptive evolution by decreasing the strength of drift. Our finding of increased genetic  
140 differentiation at range edges, which implies a restricted flow of individuals and alleles from  
141 core populations, suggests that gene flow from cores to margins is generally limited, providing  
142 additional evidence suggesting genetic swamping does not generally constrain species ranges.

143  
144 Weak support for the assumption that cores occur in the geographical center of ranges, and our  
145 finding that genetic core populations are geographically large, has likely contributed significantly  
146 to the mixed support for abundant center patterns in the literature, particularly for abundance.  
147 Tests of the abundant center hypothesis are data intensive, and syntheses of this topic have had to  
148 contend with methodological heterogeneity across studies that add statistical noise to formal  
149 meta-analyses<sup>15,20,25,26,35,36</sup>. We were able to overcome these drawbacks by harvesting publicly  
150 available genetic data, enabling us to consistently estimate metrics of genetic composition and

151 range position across disparate studies. A prominent reason why the central-marginal hypothesis  
152 has been so debated stems from differences in how range position is defined. Several continuous  
153 and categorical metrics have been used to describe range position, including distance from the  
154 range edge, the geographic range center, or the environmental niche center<sup>15,20,24</sup>. For genetic  
155 diversity in particular, studies using continuous measures of peripherality are rare<sup>15</sup>. However,  
156 our findings that core populations tend to be large suggest that it is difficult to consistently  
157 categorize range position across species. Distance from the range edge, as used here, is a  
158 continuous metric that makes no assumption about where in the range the core population lies.

159

160 We focused on mammals, and our dataset had a high concentration of samples from North  
161 America and Europe, which may affect the generalizability of our results. The predictions of the  
162 theoretical model of range edge formation we test here do not vary depending on location or  
163 species characteristics—indeed, its wide applicability is necessary for understanding whether  
164 genetic drift could be a general contributor to range edge formation. Very few species deviated  
165 from the pattern of decreased genetic diversity nearer range edges in our results (Fig. 3), and  
166 there was no tendency across genetic metrics for these species to be those sampled outside of  
167 North America or Europe. Previous work based on literature surveys, categorical measures of  
168 geographic peripherality, and distance from range centroid report find generally high support for  
169 reduced genetic diversity in range edge populations, however with variable consistency of the  
170 pattern across plants and animals<sup>15,24,37,38</sup>. The evolutionary histories and contemporary  
171 demography of individual species can contribute to variation in spatial genetic patterns in  
172 idiosyncratic ways that would introduce noise, but not bias into statistical models<sup>27,37</sup>. Thus,  
173 while our data precludes full generalization across taxa and location, there is no strong reason to

174 suspect consistent deviation from this pattern based on species traits or characteristics of species  
175 ranges.

176

### 177 **Genetic drift and range dynamics in a changing world**

178 Our empirical results align with theoretical models suggesting that the interaction between  
179 environmental gradients and the evolutionary process of genetic drift combine to produce  
180 expansion thresholds at the population level that can form distributional limits for species<sup>5,14</sup>.  
181 However, the current most widely used tool to understand and predict range dynamics is species  
182 distribution modeling<sup>39</sup>, which associates species occurrences with environments to infer suitable  
183 habitats for species as a whole. Using future climate scenarios, species distribution models are  
184 used to make predictions about how ranges will shift, expand, or contract in response to changes  
185 in the availability of suitable habitat. Species distribution models thus typically predict range  
186 dynamics as a direct outcome of species-level habitat associations while not explicitly  
187 considering evolutionary processes (see <sup>40,41</sup> for static species distribution models, but <sup>42,43</sup> for  
188 non-stationary species distribution models). Microevolutionary processes, which act on  
189 populations and can vary across species' ranges, have been shown to be important for predicting  
190 changes in species distributions<sup>44-48</sup>. Because expansion thresholds apply to populations rather  
191 than species, range dynamics in response to climate change should be highly variable and driven  
192 by intraspecific variation in population structure and environmental gradients across species  
193 ranges. For example, rapid reduction of population size and population fragmentation can cause  
194 populations to drop below the size needed for ongoing adaptation at any position in a range—not  
195 only near edges—with range-wide effects<sup>5</sup>. Conversely, deteriorating environmental conditions  
196 in core populations may increase dispersal to range edges, making genetic diversity available in  
197 edge populations and placing them above expansion thresholds<sup>5</sup>. Although poleward range shifts

198 were typically predicted to occur as species track their environmental niche, empirically, there is  
199 substantial variation in range change dynamics. Poleward shifts account for less than half of  
200 documented range movements<sup>49,50</sup>, and asymmetric changes in abundance recorded across  
201 species ranges during range shifts oppose predictions for non-evolutionary, species-level  
202 environmental tracking, and suggest population-level processes underlie range change  
203 dynamics<sup>51</sup>.

204 Establishing how microevolutionary processes contribute to macro-scale patterns in biodiversity  
205 has remained a longstanding challenge (reviewed in <sup>52,53</sup>). Species ranges are the unit of  
206 organization for higher-level biodiversity patterns, such as biodiversity hotspots, biogeographic  
207 regions, and the latitudinal richness gradient. If drift-mediated limits to range expansion stand  
208 scrutiny, they could be fundamental to our ability to forecast changes in macroecological patterns  
209 of biodiversity. Our results highlight a general mechanism by which contemporary, micro-scale,  
210 population-level demographic and evolutionary processes can contribute to the evolution of  
211 species range limits and their dynamics under global change.

212

## 213 **Methods**

### 214 Data

215 *Genetic data.* We systematically harvested publicly archived genetic data for mammal species  
216 sampled across the globe to test our questions about the contributions of population genetics to  
217 range edge formation. We expanded a database of raw microsatellite genotypes for mammal  
218 species from Canada and the USA, initially compiled between 2017-2021<sup>54,55</sup>, to cover archived  
219 data for mammals globally. For detailed methods of dataset assembly methods see Schmidt et al.  
220 <sup>54</sup>. Briefly, we obtained a list of 5216 names of species with ranges occurring outside of the

221 United States and Canada from the IUCN database to use as keywords in addition to a  
222 ‘microsat\*’ search term (e.g., *Alces alces microsat\**). We then performed a systematic search of  
223 the Dryad Digital Repository (<https://datadryad.org/stash>) by accessing the Dryad API using a  
224 custom R <sup>56</sup> script. This produced 269 results which we then manually checked for suitability,  
225 ensuring genotype data were available for the correct species, samples were collected from  
226 natural wildlife populations, the study used neutral microsatellite markers, sample design was  
227 appropriate for estimating normal levels of genetic diversity and differentiation (e.g., samples  
228 were not taken after a disturbance or recent bottleneck, if parentage analysis, offspring were  
229 excluded), and with sampling locality and population grouping information (Data S1).

230 For each sample location (local population), we recorded latitude and longitude in decimal  
231 degrees, year of sampling if applicable, and sequence of sampling (for populations sampled over  
232 time at the same location). We maintained local population groupings as delineated in the  
233 original work, and make no assumption about genetic populations or population structure. We  
234 recorded the number of loci and individuals sampled from the data directly in R. We retained  
235 local populations with at least 5 individuals sampled, and species with at least 5 local  
236 populations. The median number of individuals sampled per site across all species was 22  
237 (range: 5 – 1050 individuals; Table S1). We retained only the most recent time point for the few  
238 species with temporal sampling.

239 We estimated four metrics of genetic composition for each local population. First, we estimated  
240 gene diversity, a measure of evenness which gives the probability of randomly sampling two  
241 different alleles from a group of individuals (‘Hs’ function in the *adegenet* package<sup>57</sup>. Because  
242 gene diversity is computed from allele frequencies and not counts of alleles, it is not strongly  
243 affected by sample size<sup>58</sup>. Allelic richness was our second measure of genetic diversity. We

244 estimated rarefied allelic richness ('allelic.richness' in *hierfstat*<sup>59</sup> using 10 alleles as the  
245 minimum sample size to ensure estimates were comparable across the entire dataset. We used  
246 population-specific  $F_{ST}$  as a measure of genetic differentiation ('betas' in *hierfstat*). This metric  
247 is described in more detail in the *Mapping population structure* section below. Finally, we  
248 estimated the contemporary effective population size of the parental generation for each local  
249 population using the linkage disequilibrium method implemented in the NeEstimator software  
250 (version 2.1<sup>60</sup> accessed from R with the rLDNe package  
251 (<https://github.com/zakrobinson/RLDNe>). The linkage disequilibrium method implemented in  
252 NeEstimator is among the more accurate for estimating contemporary effective population size  
253 <sup>61</sup>, and it performs especially well for small populations. However, an estimate of infinity is  
254 returned when effective population sizes are extremely large, or when small sample size makes  
255 signals of genetic drift difficult to detect. We treated these estimates as NA values and excluded  
256 them from analysis.

257 *Range data.* We downloaded range maps from the IUCN  
258 (<https://www.iucnredlist.org/resources/spatial-data-download>). We filtered species range data  
259 based on presence, origin, and seasonality, retaining portions of the range where species  
260 populations were identified as extant, native, and resident. Many species ranges were  
261 fragmented, represented by multiple disjunct polygons. Measuring the distance of a genetic  
262 sample site to the nearest edge of a polygon thus did not necessarily represent a site's position  
263 with respect to the center and margin across an entire range. Instead, we measured the distance  
264 from each site to: 1) the nearest edge of a convex hull encompassing the species range, and 2) the  
265 geographic range centroid. We drew convex hulls and calculated centroids in the *terra* package,  
266 ensuring centroids were located within range polygons. We note that this restriction on range  
267 centroids to be inside polygon boundaries means they are not necessarily true centroids. Two

268 species, brown bears *Ursus arctos* and moose *Alces alces*, had ranges across North America and  
269 Eurasia. In these cases, we treated range polygons across continents separately and drew convex  
270 hulls and centroids for the range on each continent. We measured the geodesic distance, the  
271 shortest distance between two points along a curved surface, using the *geosphere* package in R  
272 <sup>62</sup>.

273 Although we excluded introduced populations in our genetic data where identifiable and  
274 removed portions of species ranges classified by the IUCN as *introduced*, *re-introduced*,  
275 *vagrant*, *uncertain*, or *assisted colonization*, four species had sites (22 sites in total) located  
276 outside the species' convex hull. We chose to retain these sites, as they may represent expansion  
277 not yet recorded in IUCN range data and we predicted they should nevertheless adhere to  
278 interior-marginal patterns. We made these distances negative to maintain the directionality and  
279 interpretation of our distance measure (higher values of distance indicate moving toward the  
280 range interior).

281

## 282 Bayesian hierarchical models

283 We modeled the genetic diversity and genetic differentiation in local populations as a function of  
284 range position using a series of four Bayesian generalized linear mixed models (GLMMs; 1 per  
285 genetic response variable). All response and explanatory variables were scaled and centered so  
286 that models were comparable. We expected substantial variation in mean values of genetic  
287 composition variables across species, and variation in the effect of distance to range edge across  
288 species<sup>15</sup>. We captured this structure in our models using random effects that allowed intercepts  
289 and slopes to vary across species. For each response variable we defined the linear predictor as:

$$290 y_j(s_i) = \alpha + x(s_i)\beta + \eta_j + x(s_i)\gamma_j + h_j + g(s_i) + \varepsilon_i$$

291 where  $y_j(s_i)$  is response value of species  $j$  at location  $s$  of sample  $i$ ,  $\alpha$  is the model intercept,  
292  $x(s_i)$  is distance to range edge,  $\beta$  is a fixed effect of range edge,  $\eta_j$  is the species-specific  
293 intercept,  $\gamma_j$  is species specific deviation from the fixed effect of range edge,  $h_j$  is a  
294 phylogenetically correlated species specific intercept,  $g(s_i)$  is a spatial random effect, and  $\varepsilon_i$  are  
295 the model residuals. With this model structure, we could estimate the average response ( $\beta$ ) of a  
296 genetic response variable to the distance to range edge and the random variation between species  
297 in how their responses ( $\gamma_j$ ) deviate from the average. To account for the conspecific variation in  
298 the average of a genetic metric we included independent ( $\eta_j$ ) and phylogenetically ( $h_j$ )  
299 correlated species-level random intercepts. Lastly, the locations of sample sites may cause model  
300 residuals to be spatially autocorrelated, which violates the assumptions of linear regression. We  
301 thus accounted for spatially varying intercepts by testing for spatial autocorrelation and including  
302 a spatial random effect  $g(s_i)$  when necessary. Our motivation for using a spatial random effect  
303 was only to explain the spatially correlated residual variation, not to further explore spatial  
304 variation.

305 We defined the random effects as follows:

306 The species-level random intercept and response to range edge were defined as two-dimensional  
307 correlated random effects, which are independently distributed among species. The effects are  
308 defined as:

309 
$$[\eta, \gamma] \sim N(0, W^{-1}),$$

310 where  $W^{-1}_{\eta,\eta} = 1/\tau_\eta$ ,  $W^{-1}_{\gamma,\gamma} = 1/\tau_\gamma$  and  $W^{-1}_{\eta,\gamma} = \rho/\sqrt{(\tau_\eta\tau_\gamma)}$ . The precision parameter  $\tau$   
311 captures the variance of the species-specific effects, and  $\rho$  captures their correlation. Hence, we  
312 test whether species that, on average, have higher values of a genetic response variable have a

313 larger or smaller effect of distance to range edge than an average species. In the case that  $\rho$   
314 deviates from zero, we can borrow strength across the random effects and narrow their  
315 conditional uncertainties. This method has considerable advantages over modeling each species  
316 separately because it reduces Type I error rates, and partial pooling in hierarchical models allows  
317 less well-sampled species to borrow statistical strength from better sampled species, resulting in  
318 better estimates of effect sizes. We assigned a Wishart-distribution prior with four degrees of  
319 freedom, marginal variances set to one, and correlation to zero.

320 We defined the phylogenetic random effect as a generic random effect so that

$$321 [h] \sim N(0, Q_h^{-1}),$$

322 where  $Q_h^{-1} = \tau_h C$ . The inverse correlation matrix  $C$  is the inverse of the phylogenetic distance  
323 matrix computed with the function `inverseA` from the R-package *MCMCglmm*<sup>63</sup>. The variance  
324 parameter  $\tau_h$  was assigned a penalized complexity prior which gives a 0.1 prior probability that  
325 the standard deviation of  $h$  ( $= \tau_h^{-1/2}$ ) has a value larger than one. This is a relatively vague  
326 prior. We also fit models without a phylogenetic random effect to test the sensitivity of our  
327 results to the inclusion of the phylogeny (Table S3).

328 Lastly, we defined the spatial random effect as a Besag-type random effect, for which the value  
329 in a location is an average of the values of the adjacent sampling locations<sup>64</sup>. The random effect  
330 at location  $s$  conditional on connected study location is defined as

$$331 g(s_i) | g(s_{-i}) \sim N(\mu(s_i), Q_g^{-1}),$$

332 where  $\mu(s_i)$  is the average over the  $g$  in the nearby study locations and  $Q_g^{-1} = 1/N\tau_g$ .  $N$  is the  
333 number of connected study locations and  $\tau_g$  is the precision parameter. We assigned it a  
334 penalized complexity prior which gives a 0.1 prior probability that the standard deviation of  $g$  ( $=$

335  $\tau_g^{-1/2}$ ) has a value larger than one. We defined the connectivity structure of the study sites with  
336 a k-nearest neighbor method by fixing the number of neighbors per site to 4 for effective  
337 population size, 6 for population-specific  $F_{ST}$ , 8 for gene diversity, and 2 for allelic richness. We  
338 chose these connectivity structures by running model candidates with numbers of connections  
339 per site varying from 1 to 8 and comparing them to models with no spatial random effect. The k-  
340 nearest neighbor is an unsupervised algorithm which assigns connections between sites  
341 according to *a priori* rules. It considers only the geographical distances between sites and does  
342 not consider oceans or biogeographic regions which could affect the genetic metrics. We visually  
343 inspected all candidate connectivity structures to ensure they captured the neighborhood  
344 structures on each continent and avoided between-continent connections. We measured spatial  
345 autocorrelation with the probability that the Moran Index of residuals deviated from zero, and  
346 excluded models with spatially correlated residuals. Of the remaining model candidates, we  
347 chose the model with the best information content according to WAIC<sup>65</sup> (Table S4).

348 We ran parallel analyses with the same model structure and selection procedure with distance to  
349 range centroid as an explanatory variable instead of distance to range edge. We fit all models in  
350 R version 4.1.2 using the integrated nested Laplace approximation with the INLA package<sup>66</sup>. We  
351 computed marginal and conditional  $R^2$  values for mixed-effects models as additional indicators  
352 of model fit (Table S2)<sup>67,68</sup>. Marginal and conditional  $R^2$  partition the variance explained by a  
353 model into the component explained by fixed effects only (marginal  $R^2$ ) and that explained by  
354 both fixed and random effects (conditional  $R^2$ ).

355

356 Mapping population structure

357 We explored spatial patterns of genetic differentiation for species using an approach from Kitada  
358 et al.<sup>32</sup> that combines estimates of population-specific  $F_{ST}$  and pairwise  $F_{ST}$  to characterize spatial  
359 population structure. Population-specific  $F_{ST}$ <sup>31</sup> is a measure of population divergence estimated  
360 for individual samples—not pairs of samples—that uses proportions of matching alleles for pairs  
361 of alleles drawn from within and between populations to estimate differentiation. Population-  
362 specific  $F_{ST}$  describes the decay in genetic diversity and similarity from the most diverse local  
363 population, which is what we were interested in mapping and modeling. Because it is an estimate  
364 of differentiation relative to a single, most diverse sample, population-specific  $F_{ST}$  does not  
365 provide information about how differentiated sample sites are relative to each other. For this, we  
366 use pairwise  $F_{ST}$ . Combining population-specific  $F_{ST}$ , pairwise  $F_{ST}$ , and spatial metadata can  
367 provide a general idea about regions with large populations well-connected by gene flow that  
368 may represent the “core” areas of a species range. We estimated both  $F_{ST}$  metrics in the hierfstat  
369 package, using the ‘pairwise.neifst’ function to estimate Nei and Chesser’s pairwise  $G_{ST}$ <sup>69</sup>, and  
370 ‘betas’ to estimate population-specific  $F_{ST}$ .

371 To visualize patterns of genetic diversity decay and genetic differentiation, we generated 2 plots  
372 per species to represent population structure in complementary ways (Fig. 4, Fig. S7); for a  
373 detailed description of these methods see <sup>32</sup>. We focused on 12 species that had good coverage of  
374 their range. The first plot showed population-specific  $F_{ST}$  values across species’ ranges. To  
375 visualize the major axes of genetic differentiation, we performed a principal coordinates analysis  
376 (PCoA) on the pairwise genetic differentiation matrix and plotted site positions on the first two  
377 PCoA axes.

378

379 **Acknowledgments:** We thank Sean Robertson, Leah Kathan, Jessie Ogden, and Meghan  
380 Mahoney for early discussions on this topic. We also thank the Population Ecology and  
381 Evolutionary Genetics group and the Evolutionary Biology BIOL 3300 students at the University  
382 of Manitoba for their comments and feedback on manuscript drafts. C.S. acknowledges the  
383 support of iDiv funded by the German Research Foundation (DFG–FZT 118, 202548816) and a  
384 Natural Sciences and Engineering Research Council of Canada Discovery Grant. C.G. was  
385 supported by a Natural Sciences and Engineering Research Council of Canada Discovery Grant.

386

387 **Author contributions:**

388 Conceptualization: CS, CJG, JPL

389 Methodology: CS, JM, CJG

390 Investigation: CS

391 Formal analysis: CS, JM

392 Visualization: CS

393 Writing – original draft: CS, CG

394 Writing – review and editing: all authors

395 Funding acquisition: CS, CJG

396

397 **Data and code availability:** All data underlying this work are publicly available (Table S1).

398 Analysis code is available at: [https://github.com/chloewsch/range\\_edge\\_genetics](https://github.com/chloewsch/range_edge_genetics).

399

400 **References**

401 1. Antonovics, J. The Input from Population Genetics: ‘The New Ecological Genetics’.

402 *Systematic Botany* **1**, 233–245 (1976).

403 2. Bradshaw, A. D. Genostasis and the Limits to Evolution. *Philosophical Transactions:*

404 *Biological Sciences* **333**, 289–305 (1991).

405 3. Bridle, J. R. & Vines, T. H. Limits to evolution at range margins: when and why does

406 adaptation fail? *Trends in Ecology and Evolution* **22**, 140–147 (2007).

407 4. Gaston, K. J. *The Structure and Dynamics of Geographic Ranges*. (Oxford University Press,

408 Oxford, 2003).

- 409 5. Polechová, J. Is the sky the limit? On the expansion threshold of a species' range. *PLOS*  
410 *Biology* **16**, e2005372 (2018).
- 411 6. Gillespie, J. H. *The Causes of Molecular Evolution*. (Oxford University Press, New York,  
412 2002).
- 413 7. Polechová, J., Barton, N. & Marion, G. Species' range: adaptation in space and time. *The*  
414 *American Naturalist* **174**, E186-204 (2009).
- 415 8. Kirkpatrick, M. & Barton, N. Evolution of a species' range. *The American Naturalist* **150**, 1–  
416 23 (1997).
- 417 9. Polechová, J. & Barton, N. H. Limits to adaptation along environmental gradients.  
418 *Proceedings of the National Academy of Sciences of the United States of America* **112**,  
419 6401–6406 (2015).
- 420 10. Waples, R. S. What is Ne, anyway? *Journal of Heredity* **113**, 371–379 (2022).
- 421 11. Ohta, T. The Nearly Neutral Theory of Molecular Evolution. *Annual Review of Ecology and*  
422 *Systematics* **23**, 263–286 (1992).
- 423 12. Kimura, M. *The Neutral Theory of Molecular Evolution*. (Cambridge University Press,  
424 Cambridge, 1983).
- 425 13. Marino, A., Debaecker, G., Fiston-Lavier, A.-S., Haudry, A. & Nabholz, B. Effective  
426 population size does not explain long-term variation in genome size and transposable  
427 element content in animals. *eLife* **13**, RP100574 (2025).
- 428 14. Connallon, T. & Sgrò, C. M. In search of a general theory of species' range evolution. *PLoS*  
429 *Biology* **16**, 1–6 (2018).
- 430 15. Eckert, C. G., Samis, K. E. & Loughheed, S. C. Genetic variation across species' geographical  
431 ranges: The central-marginal hypothesis and beyond. *Molecular Ecology* **17**, 1170–1188  
432 (2008).

- 433 16. Bridle, J. R., Kawata, M. & Butlin, R. K. Local adaptation stops where ecological gradients  
434 steepen or are interrupted. *Evolutionary Applications* 1–14 (2019) doi:10.1111/eva.12789.
- 435 17. Charlesworth, B. Effective population size and patterns of molecular evolution and variation.  
436 *Nature Reviews Genetics* **10**, 195–205 (2009).
- 437 18. Brown, J. H. On the Relationship between Abundance and Distribution of Species. *The*  
438 *American Naturalist* **124**, 255–279 (1984).
- 439 19. Dallas, T., Decker, R. R. & Hastings, A. Species are not most abundant in the centre of their  
440 geographic range or climatic niche. *Ecology Letters* **20**, 1526–1533 (2017).
- 441 20. Fristoe, T. S., Vilela, B., Brown, J. H. & Botero, C. A. Abundant-core thinking clarifies  
442 exceptions to the abundant-center distribution pattern. *Ecography* 1–15 (2022)  
443 doi:10.1111/ecog.06365.
- 444 21. Hargreaves, A. L., Samis, K. E. & Eckert, C. G. Are species' range limits simply niche limits  
445 writ large? A review of transplant experiments beyond the range. *American Naturalist* **183**,  
446 157–173 (2014).
- 447 22. Kottler, E. J., Dickman, E. E., Sexton, J. P., Emery, N. C. & Franks, S. J. Draining the  
448 Swamping Hypothesis: Little Evidence that Gene Flow Reduces Fitness at Range Edges.  
449 *Trends in Ecology and Evolution* **36**, 533–544 (2021).
- 450 23. Lee-Yaw, J. A. *et al.* A synthesis of transplant experiments and ecological niche models  
451 suggests that range limits are often niche limits. *Ecology Letters* **19**, 710–722 (2016).
- 452 24. Pironon, S. *et al.* Geographic variation in genetic and demographic performance: new  
453 insights from an old biogeographical paradigm. *Biological Reviews* **92**, 1877–1909 (2017).
- 454 25. Sagarin, R. D. & Gaines, S. D. The 'abundant centre' distribution: To what extent is it a  
455 biogeographical rule? *Ecology Letters* **5**, 137–147 (2002).

- 456 26. Santini, L., Pironon, S., Maiorano, L. & Thuiller, W. Addressing common pitfalls does not  
457 provide more support to geographical and ecological abundant-centre hypotheses. *Ecography*  
458 **42**, 696–705 (2019).
- 459 27. Singhal, S., Wrath, J. & Rabosky, D. L. Genetic variability and the ecology of geographic  
460 range: A test of the central-marginal hypothesis in Australian scincid lizards. *Molecular*  
461 *Ecology* **31**, 4242–4253 (2022).
- 462 28. Rolland, J., Lavergne, S. & Manel, S. Combining niche modelling and landscape genetics to  
463 study local adaptation: A novel approach illustrated using alpine plants. *Perspectives in*  
464 *Plant Ecology, Evolution and Systematics* **17**, 491–499 (2015).
- 465 29. Ledoux, J.-B. *et al.* Potential for adaptive evolution at species range margins: contrasting  
466 interactions between red coral populations and their environment in a changing ocean.  
467 *Ecology and Evolution* **5**, 1178–1192 (2015).
- 468 30. Nei, M. *Molecular Evolutionary Genetics*. (Columbia University Press, New York  
469 Chichester, West Sussex, 1987).
- 470 31. Weir, B. S. & Goudet, J. A Unified Characterization of Population Structure and  
471 Relatedness. *Genetics* **206**, 2085–2103 (2017).
- 472 32. Kitada, S., Nakamichi, R. & Kishino, H. Understanding population structure in an  
473 evolutionary context: Population-specific FST and pairwise FST. *G3: Genes, Genomes,*  
474 *Genetics* **11**, (2021).
- 475 33. Haldane, J. B. S. The relation between density regulation and natural selection. *Proceedings*  
476 *of the Royal Society of London. Series B - Biological Sciences* **145**, 306–308 (1956).
- 477 34. Polechová, J. The costs and benefits of dispersal in small populations. *Philosophical*  
478 *Transactions of the Royal Society B: Biological Sciences* **377**, 2021.12.16.472951 (2022).

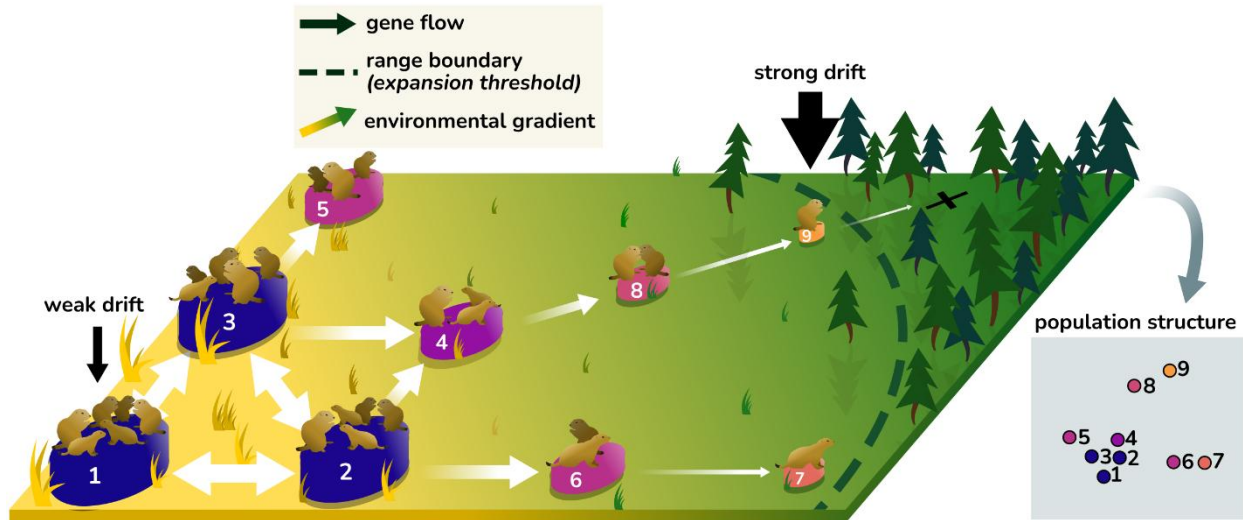
- 479 35. Sagarin, R. D., Gaines, S. D. & Gaylord, B. Moving beyond assumptions to understand  
480 abundance distributions across the ranges of species. *Trends in Ecology and Evolution* **21**,  
481 524–530 (2006).
- 482 36. Soberón, J., Peterson, A. T. & Osorio-Olvera, L. A comment on “Species are not most  
483 abundant in the centre of their geographic range or climatic niche”. *Rethinking Ecology* **3**,  
484 13–18 (2018).
- 485 37. De Kort, H. *et al.* Life history, climate and biogeography interactively affect worldwide  
486 genetic diversity of plant and animal populations. *Nature Communications* **12**, 516 (2021).
- 487 38. Lira-Noriega, A. & Manthey, J. D. Relationship of genetic diversity and niche centrality: A  
488 survey and analysis. *Evolution* **68**, 1082–1093 (2014).
- 489 39. Guisan, A. & Thuiller, W. Predicting species distribution: offering more than simple habitat  
490 models. *Ecology Letters* **8**, 993–1009 (2005).
- 491 40. A. Lee-Yaw, J., L. McCune, J., Pironon, S. & N. Sheth, S. Species distribution models rarely  
492 predict the biology of real populations. *Ecography* **2022**, 1–16 (2022).
- 493 41. Zurell, D., Jeltsch, F., Dormann, C. F. & Schröder, B. Static species distribution models in  
494 dynamically changing systems: how good can predictions really be? *Ecography* **32**, 733–744  
495 (2009).
- 496 42. Benito Garzón, M., Alía, R., Robson, T. M. & Zavala, M. A. Intra-specific variability and  
497 plasticity influence potential tree species distributions under climate change. *Global Ecology*  
498 *and Biogeography* **20**, 766–778 (2011).
- 499 43. Hällfors, M. H. *et al.* Addressing potential local adaptation in species distribution models:  
500 implications for conservation under climate change. *Ecological Applications* **26**, 1154–1169  
501 (2016).

- 502 44. Bay, R. A. *et al.* Genomic signals of selection predict climate-driven population declines in a  
503 migratory bird. *Science* **359**, 83–86 (2018).
- 504 45. Fitzpatrick, M. C., Chhatre, V. E., Soolanayakanahally, R. Y. & Keller, S. R. Experimental  
505 support for genomic prediction of climate maladaptation using the machine learning  
506 approach Gradient Forests. *Molecular Ecology Resources* **21**, 2749–2765 (2021).
- 507 46. Jay, F. *et al.* Forecasting changes in population genetic structure of alpine plants in response  
508 to global warming. *Molecular Ecology* **21**, 2354–2368 (2012).
- 509 47. D’Amen, M. & Azzurro, E. Integrating univariate niche dynamics in species distribution  
510 models: A step forward for marine research on biological invasions. *Journal of*  
511 *Biogeography* **47**, 686–697 (2020).
- 512 48. Hanspach, J., Kühn, I., Schweiger, O., Pompe, S. & Klotz, S. Geographical patterns in  
513 prediction errors of species distribution models: Patterns in prediction error. *Global Ecology*  
514 *and Biogeography* **20**, 779–788 (2011).
- 515 49. Platts, P. J. *et al.* Habitat availability explains variation in climate-driven range shifts across  
516 multiple taxonomic groups. *Scientific Reports* **9**, 1–10 (2019).
- 517 50. Rubenstein, M. A. *et al.* Climate change and the global redistribution of biodiversity:  
518 substantial variation in empirical support for expected range shifts. *Environmental Evidence*  
519 1–21 (2023) doi:10.1186/s13750-023-00296-0.
- 520 51. Chaikin, S., Riva, F., Marshall, K. E., Lessard, J.-P. & Belmaker, J. Marine fishes  
521 experiencing high-velocity range shifts may not be climate change winners. *Nat Ecol Evol* **8**,  
522 936–946 (2024).
- 523 52. Charlesworth, B., Lande, R. & Slatkin, M. A Neo-Darwinian Commentary on  
524 Macroevolution. *Evolution* **36**, 474 (1982).

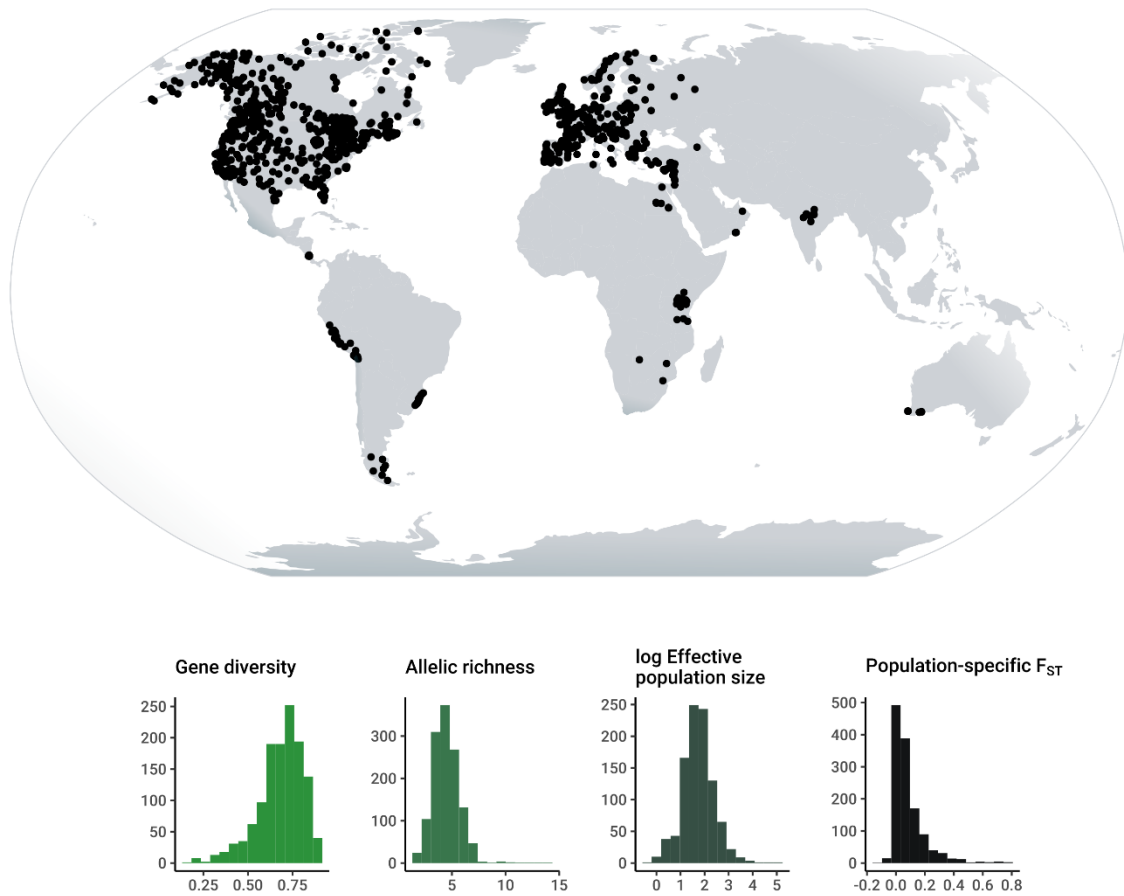
- 525 53. Hancock, Z. B., Lehmborg, E. S. & Bradburd, G. S. Neo-darwinism still haunts evolutionary  
526 theory: A modern perspective on Charlesworth, Lande, and Slatkin (1982). *Evolution* **75**,  
527 1244–1255 (2021).
- 528 54. Schmidt, C., Domaratzki, M., Kinnunen, R. P., Bowman, J. & Garroway, C. J. Continent-  
529 wide effects of urbanization on bird and mammal genetic diversity. *Proceedings of the Royal*  
530 *Society B: Biological Sciences* **287**, 20192497 (2020).
- 531 55. Schmidt, C. & Garroway, C. J. Systemic racism alters wildlife genetic diversity. *Proceedings*  
532 *of the National Academy of Sciences of the United States of America* **119**, 0–3 (2022).
- 533 56. R Core Team. R: A Language and Environment for Statistical Computing. (2021).
- 534 57. Jombart, T. *et al.* adegenet: Exploratory Analysis of Genetic and Genomic Data. (2017).
- 535 58. Charlesworth, B. & Charlesworth, D. *Elements of Evolutionary Genetics*. (Roberts &  
536 Company Publishers, Greenwood Village, Colorado, USA, 2010).
- 537 59. Goudet, J. & Jombart, T. hierfstat: Estimation and Tests of Hierarchical F-Statistics. (2015).
- 538 60. Do, C. *et al.* NeEstimator v2: Re-implementation of software for the estimation of  
539 contemporary effective population size ( $N_e$ ) from genetic data. *Molecular Ecology*  
540 *Resources* **14**, 209–214 (2014).
- 541 61. Gilbert, K. J. & Whitlock, M. C. Evaluating methods for estimating local effective  
542 population size with and without migration. *Evolution* **69**, 2154–2166 (2015).
- 543 62. Hijmans, R. J. geosphere: Spherical Trigonometry. (2019).
- 544 63. Hadfield, J. MCMC GLMM. (2018).
- 545 64. Besag, J. Spatial Interaction and the Statistical Analysis of Lattice Systems. *Journal of the*  
546 *Royal Statistical Society: Series B (Methodological)* **36**, 192–225 (1974).
- 547 65. Gelman, A., Hwang, J. & Vehtari, A. Understanding predictive information criteria for  
548 Bayesian models. *Stat Comput* **24**, 997–1016 (2014).

- 549 66. Lindgren, F. & Rue, H. Bayesian spatial modelling with R-INLA. *Journal of Statistical*  
550 *Software* **63**, 1–25 (2015).
- 551 67. Nakagawa, S. & Schielzeth, H. A general and simple method for obtaining R<sup>2</sup> from  
552 generalized linear mixed-effects models. *Methods in Ecology and Evolution* **4**, 133–142  
553 (2013).
- 554 68. Johnson, P. C. D. Extension of Nakagawa & Schielzeth's R<sup>2</sup>GLMM to random slopes  
555 models. *Methods in Ecology and Evolution* **5**, 944–946 (2014).
- 556 69. Nei, M. & Chesser, R. K. Estimation of fixation indices and gene diversities. *Annals of*  
557 *Human Genetics* **47**, 253–259 (1983).
- 558

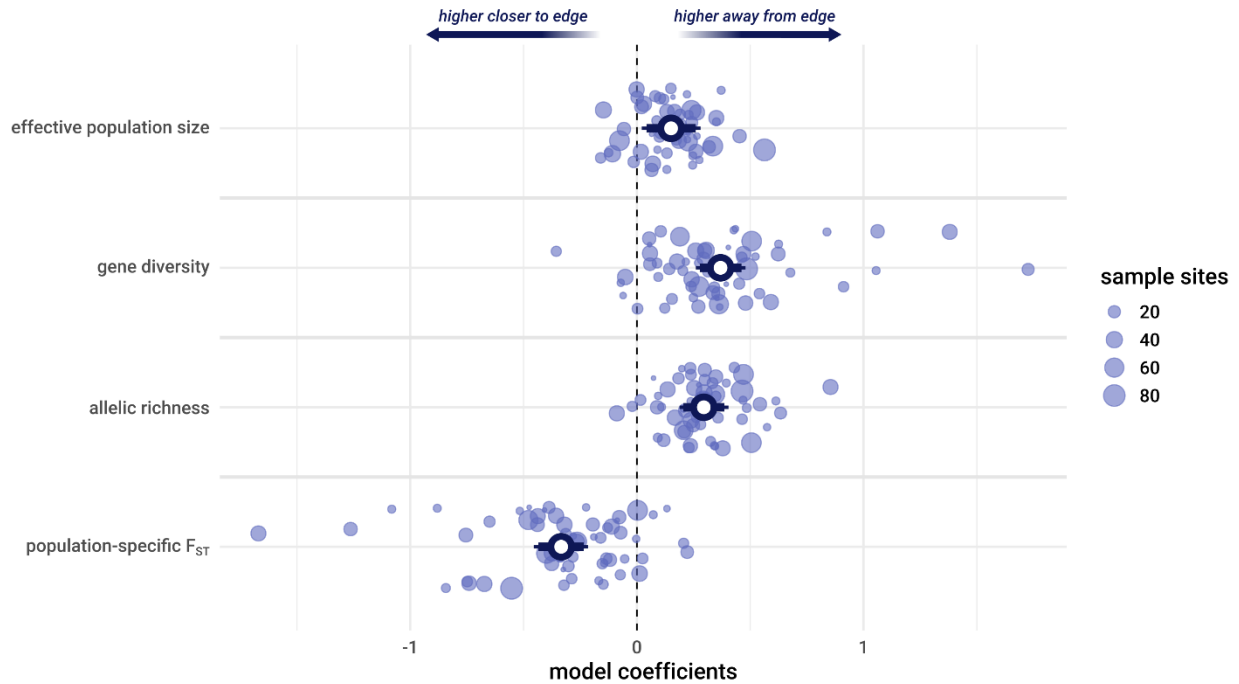
559



560 **Fig. 1. Hypothesized conceptual model of drift-limited range expansion.** Population sizes are  
561 larger and more well-connected toward the range interior where environments are more suitable  
562 (populations 1-3). As the environment changes, populations become smaller, more isolated, and  
563 more genetically differentiated (populations 4-9). Expansion thresholds form when populations  
564 are so small that genetic drift overwhelms natural selection and adaptation is no longer possible  
565 (populations 7 and 9).  
566



567 **Fig. 2. Overview of genetic data.** The map shows the spatial distribution of genetic data from  
 568 1271 sample locations of 59 mammal species (see species-specific maps in Fig. S1). Histograms  
 569 show the distribution and range of values for each metric of genetic composition: gene diversity  
 570 and allelic richness are metrics of diversity, effective population size measures the strength of  
 571 genetic drift, and population-specific  $F_{ST}$  (fixation index) is a measure of genetic differentiation.  
 572

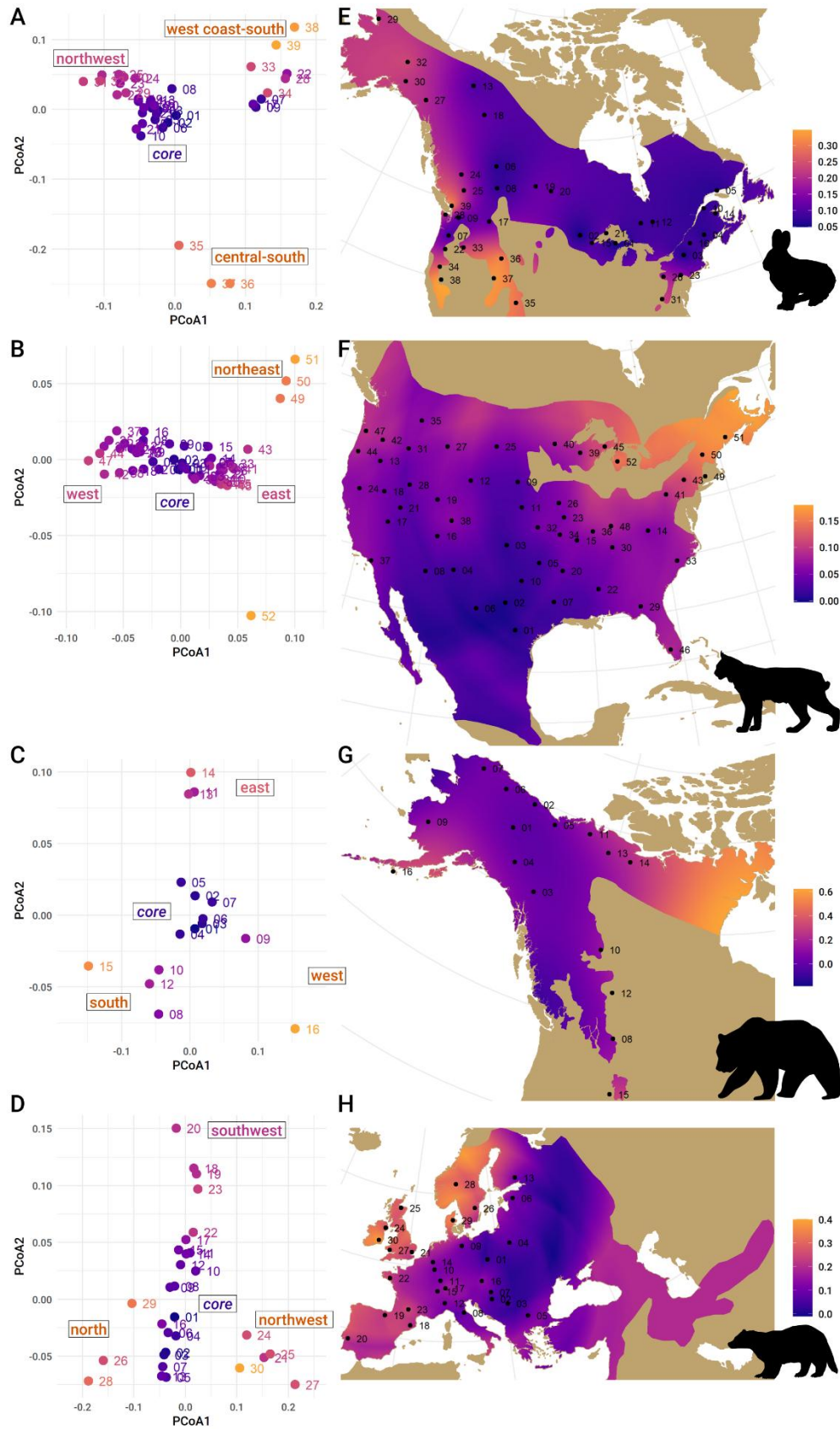


573 **Fig. 3. Variation in genetic diversity and differentiation across species ranges.** Model  
 574 coefficients of the relationship between range position (distance to the edge of range convex  
 575 hull) and each genetic metric (y axis) from Bayesian generalized mixed models controlling for  
 576 the spatial distribution of sites and species relatedness. Effective population size is a  
 577 contemporary effective size estimated using the linkage disequilibrium method for single-  
 578 samples (SI Methods). Gene diversity and allelic richness (rarefied) are two metrics of genetic  
 579 diversity. Population-specific  $F_{ST}$  is a measure of genetic differentiation that estimates how far  
 580 single populations have diverged from a common ancestor of all sites in the sample. Open circles  
 581 represent the relationship between range position and genetic metrics across all species with 90%  
 582 (thin lines) and 95% (thick lines) credible intervals. Filled circles are estimated species-specific  
 583 relationships between range position and the genetic metrics. The dashed vertical line indicates  
 584 an effect size of 0. Positive effect sizes indicate genetic diversity and connectivity increase with  
 585 increasing distance from the range edge, while negative effect sizes mean genetic diversity is  
 586 reduced and local populations are more differentiated closer to the range edge.

587

588

589



590 **Fig. 4. Patterns of range-wide population differentiation.** Spatial population structure is

591 mapped for species with whole range coverage: snowshoe hare (*Lepus americanus*), bobcat  
592 (*Lynx rufus*), grizzly bear (*Ursus arctos*), and Eurasian badger (*Meles meles*); see Fig S4 for  
593 additional species. Colors represent population-specific  $F_{ST}$  values, with darker blue colors  
594 depicting local populations that are the most genetically similar to the most diverse local  
595 population compared to orange colored sites, which are the most strongly genetically  
596 differentiated. Plots (A-D) show major axes of population differentiation from a principal  
597 coordinates analyses (PCoA) of Nei's pairwise- $F_{ST}$ , which measures the magnitude of genetic  
598 differentiation between pairs of local populations. The central location of genetic core  
599 populations with low differentiation in PCoA plots suggest they are well-connected by gene  
600 flow. Labels indicate spatial direction of differentiation that correspond to maps in (E-H). Large  
601 dark blue areas across maps suggests that larger, well-connected core populations can cover large  
602 proportions of the species range and are not limited to the geographic range center.  
603

604 **Table 1. Summaries of Bayesian hierarchical models relating genetic metrics to range**  
605 **position.** The effect size of range position is given with 95% credible intervals. Range position is  
606 described by the distance to the edge of the range convex hull. Models controlled for spatial and  
607 phylogenetic correlation.  $\sigma_{\text{intercept}}$  is the standard deviation of species-specific intercepts, and  
608 summarizes variation in mean genetic diversity, effective population size, or  $F_{ST}$  across species.  
609  $\sigma_{\text{slope}}$  is the standard deviation of species-specific estimates of the effect of distance, and shows  
610 variation in species responses to range position. Marginal log-likelihood and DIC (Deviance  
611 Information Criterion) are two model fit metrics.

612

Variable	Range position	$\sigma_{\text{intercept}}$	$\sigma_{\text{slope}}$	Marginal log likelihood	WAIC
gene diversity	0.37 (0.26 – 0.48)	0.79 (0.59 – 1.03)	0.48 (0.36 – 0.64)	-1912.16	1635.06
allelic richness	0.30 (0.19 – 0.40)	0.66 (0.47 – 0.93)	0.32 (0.24 – 0.44)	-1795.71	2895.87
effective population size	0.15 (0.02 – 0.28)	0.41 (0.31 – 0.53)	0.33 (0.23 – 0.45)	-1939.89	2511.31
population-specific $F_{ST}$	-0.33 (-0.45 – -0.22)	0.56 (0.41 – 0.78)	0.48 (0.35 – 0.64)	-2300.26	2614.05

613